Electronic Supplementary Material (ESI) for Journal of Materials Chemistry A.

Computational Screening of Two-Dimensional Conductive Metal-Organic Frameworks as Electrocatalysts for Nitric Oxide Reduction Reaction

Man Qiao,[*a] *Ye Yue,*[b] *Jiachi Xie*[a] *and Dongdong Zhu*[*a]

[a] School of Chemistry and Materials Science, Institute of Advanced Materials and Flexible Electronics (IAMFE), Nanjing University of Information Science and Technology, Nanjing 210044, China.
E-mail: dd.zhu@nuist.edu.cn, qiaoman@nuist.edu.cn

[b] Reading Academy, Nanjing University of Information Science and Technology, Nanjing 210044, China

Table S1. Structural parameters, formation energy and the dissolution energy of $TM_3(C_6O_6)$.

M=	Lattice (Å)	$D_{M\text{-}M}$ (Å)	$D_{M\text{-}O}$ (Å)	E_{form} (eV)	U_{diss} (eV)
Sc	13.93	6.99	2.05	-6.55	0.10
Ti	13.52	6.77	1.91	-5.21	0.98
V	13.46	6.73	1.88	-3.98	0.81
Cr	13.34	6.69	1.94	-3.95	1.07
Mn	13.16	6.58	1.88	-4.33	0.98
Fe	13.06	6.53	1.86	-2.17	0.63
Co	12.94	6.47	1.83	-2.18	0.81
Ni	12.88	6.44	1.83	-2.31	0.90
Cu	13.21	6.60	1.95	-1.81	1.25
Y	14.40	7.19	2.17	-6.49	-0.21
Zr	14.05	7.02	2.04	-5.39	-0.1
Nb	13.85	6.92	1.98	-4.07	0.26
Mo	13.77	6.89	1.98	-2.56	0.65
Ru	13.54	6.77	1.96	-1.46	1.19
Rh	13.46	6.73	1.98	-1.55	1.37
Pd	13.41	6.70	1.99	-1.59	1.74
Ag	14.50	7.26	2.27	-0.73	1.53
Hf	13.95	6.97	2.03	-5.08	-0.28
Ta	13.8	6.90	1.97	-3.97	0.72
W	13.8	6.90	1.97	-1.45	0.58
Re	13.8	6.90	1.99	-0.60	0.50
Os	13.64	6.82	1.95	-0.69	0.93
Ir	13.59	6.79	1.98	-0.73	1.40
Pt	13.52	6.76	1.98	-1.19	1.77
Au	13.45	6.73	1.99	0.06	1.48

Table S2. The Gibbs free energies of NO (ΔG_{*NO}), N_2 molecule (ΔG_{*N2}), and NH_3 molecule (ΔG_{*NH3}) on $TM_3(C_6O_6)_2$.

M=	ΔG_{ad} (NO) (eV)	ΔG_{ad} (N_2) (eV)	ΔG_{ad} (NH_3) (eV)
Ti	-0.38	0.08	-0.50
V	-1.35	0.29	-0.75
Cr	-1.61	0.02	-1.30
Mn	-0.70	0.47	-0.66
Fe	-1.19	0.46	-0.75
Co	-1.01	0.23	-0.97
Nb	-4.69	-0.57	-0.60
Mo	-2.65	-0.47	-1.59
Ru	-2.06	-0.29	-1.14
Rh	-1.45	0.4	-1.13
W	-3.01	0.49	-1.46
Re	-2.60	-0.21	-1.18
Os	-2.24	-0.06	-0.95
Ir	-1.47	0.52	-1.19

Table S3. The Gibbs free energies (ΔG_{*NO}), N-O bond, N-N bond and transfer charge of TM atoms of adsorbed NO on $TM_3(C_6O_6)_2$

M=	ΔG_{ad} (NO) (eV)	L_{N-O} (Å)	D_{M-N} (Å)	Charge (|e|)
V	-1.35	1.22	1.69	0.42
Cr	-1.61	1.19	1.66	0.26
Mn	-0.70	1.19	1.63	0.23
Fe	-1.19	1.18	1.64	0.11
Co	-1.01	1.17	1.65	0.13
Nb	-4.69	1.26	1.82	0.56
Mo	-2.65	1.22	1.74	0.53
Ru	-2.06	1.18	1.71	0.28
Rh	-1.45	1.18	1.93	0.12
W	-3.01	1.23	1.75	0.57
Re	-2.60	1.20	1.73	0.46
Os	-2.24	1.19	1.72	0.26
Ir	-1.47	1.19	1.94	0.16

Table S4. Elementary steps for the considered pathways of NO-to-NH_3 conversion on nine $TM_3(C_6O_6)_2$.

ΔG (eV)	V	Mn	Fe	Mo	Ru
$*NO + H^+ + e^- \rightarrow *NOH$	0.49	0.60	0.80	/	0.20
$*NO + H^+ + e^- \rightarrow *NHO$	0.20	0.02	0.28	0.01	0.61
$*NOH + H^+ + e^- \rightarrow *N + H_2O$	-1.15	-1.12	-0.45	/	-1.59
$*NOH + H^+ + e^- \rightarrow *NHOH$	-0.55	-0.13	-0.35	/	-0.11
$*NHO + H^+ + e^- \rightarrow *NHOH$	-0.26	0.46	0.18	0.04	-0.51
$*NHO + H^+ + e^- \rightarrow *NH_2O$	0.28	-0.10	0.07	-0.19	-1.02
$*N + H^+ + e^- \rightarrow *NH$	-0.88	-0.02	-0.54	-0.68	-0.36
$*NHOH + H^+ + e^- \rightarrow *NH_2OH$	0.08	-1.24	-0.84	-1.05	0.22
$*NHOH + H^+ + e^- \rightarrow *NH + H_2O$	-1.47	-1.01	-0.65	0.36	-1.85
$*NH_2O + H^+ + e^- \rightarrow *NH_2OH$	-0.46	-0.68	-0.72	-0.83	0.72
$*NH + H^+ + e^- \rightarrow *NH_2$	-0.73	-1.40	-1.46	-2.03	-0.31
$*NH_2OH + H^+ + e^- \rightarrow *NH_2 + H_2O$	-2.28	-1.16	-1.27	-0.62	-2.37
$*NH_2 + H^+ + e^- \rightarrow *NH_3$	-0.61	-1.50	-1.37	-1.80	-0.35
$*NH_3 \rightarrow * + NH_3$	0.73	0.64	0.73	0.95	1.57
$* + H^+ + e^- \rightarrow *H$	0.47	0.70	0.71	0.17	-0.36

ΔG (eV)	Rh	W	Ir	Co
$*NO + H^+ + e^- \rightarrow *NOH$	0.65	0.72	0.07	/
$*NO + H^+ + e^- \rightarrow *NHO$	0.23	0.26	0.58	0.02
$*NOH + H^+ + e^- \rightarrow *N + H_2O$	-1.36	2.08	-1.34	/
$*NOH + H^+ + e^- \rightarrow *NHOH$	-0.29	-0.51	0.05	/
$*NHO + H^+ + e^- \rightarrow *NHOH$	0.13	-0.05	-0.45	0.19
$*NHO + H^+ + e^- \rightarrow *NH_2O$	0.63	-0.22	-1.05	0.20
$*N + H^+ + e^- \rightarrow *NH$	0.40	-3.01	-0.79	/
$*NHOH + H^+ + e^- \rightarrow *NH_2OH$	-0.49	-0.91	0.68	-1.00
$*NHOH + H^+ + e^- \rightarrow *NH + H_2O$	-0.68	-0.42	-2.18	/
$*NH_2O + H^+ + e^- \rightarrow *NH_2OH$	-0.99	-0.74	1.28	-1.02
$*NH + H^+ + e^- \rightarrow *NH_2$	-1.18	-1.14	-0.15	/
$*NH_2OH + H^+ + e^- \rightarrow *NH_2 + H_2O$	-1.37	-0.66	-3.00	-0.90
$*NH_2 + H^+ + e^- \rightarrow *NH_3$	-1.06	-1.79	0.28	-1.49
$*NH_3 \rightarrow * + NH_3$	1.12	1.11	1.44	1.17
$* + H^+ + e^- \rightarrow *H$	0.65	0.72	0.07	/

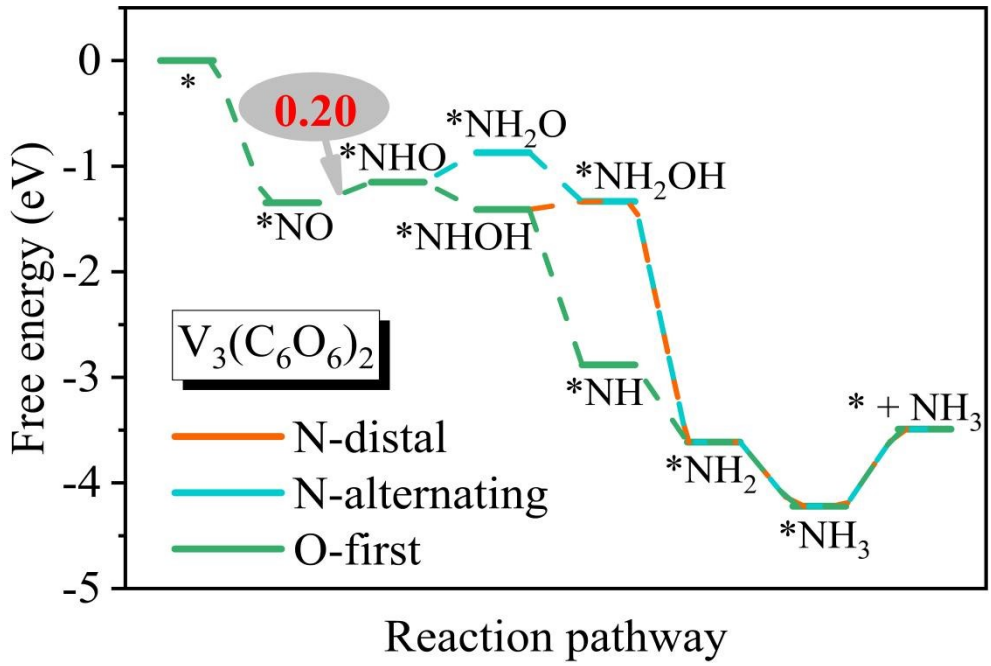

Fig. S1. The free energy diagram of NO reduction to NH_3 on $V_3(C_6O_6)_2$.

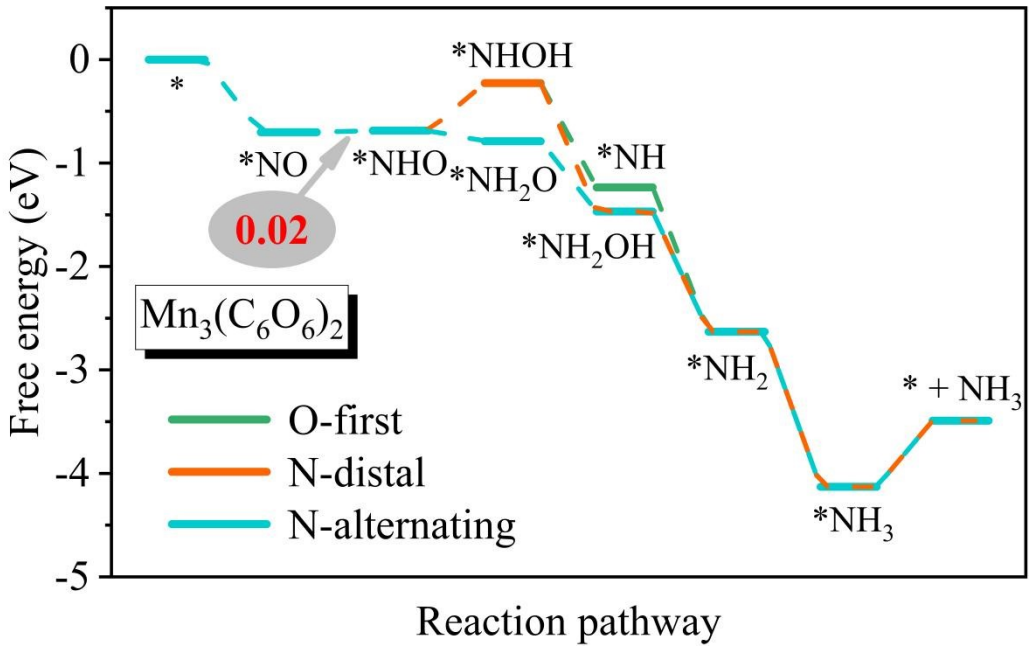

Fig. S2. The free energy diagram of NO reduction to NH_3 on $Mn_3(C_6O_6)_2$.

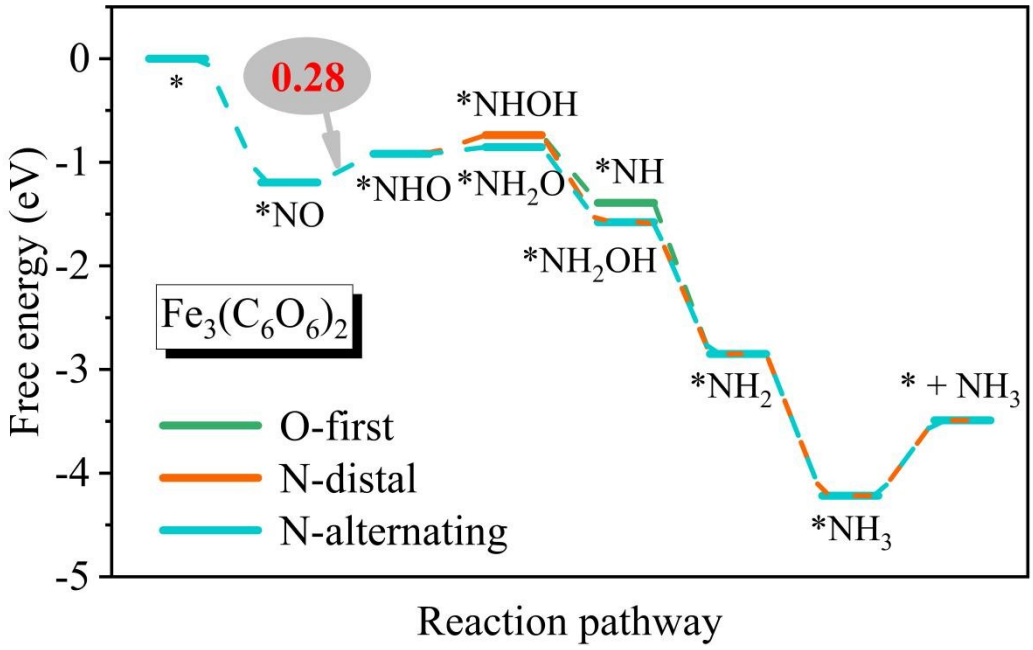

Fig. S3. The free energy diagram of NO reduction to NH_3 on $Mn_3(C_6O_6)_2$.

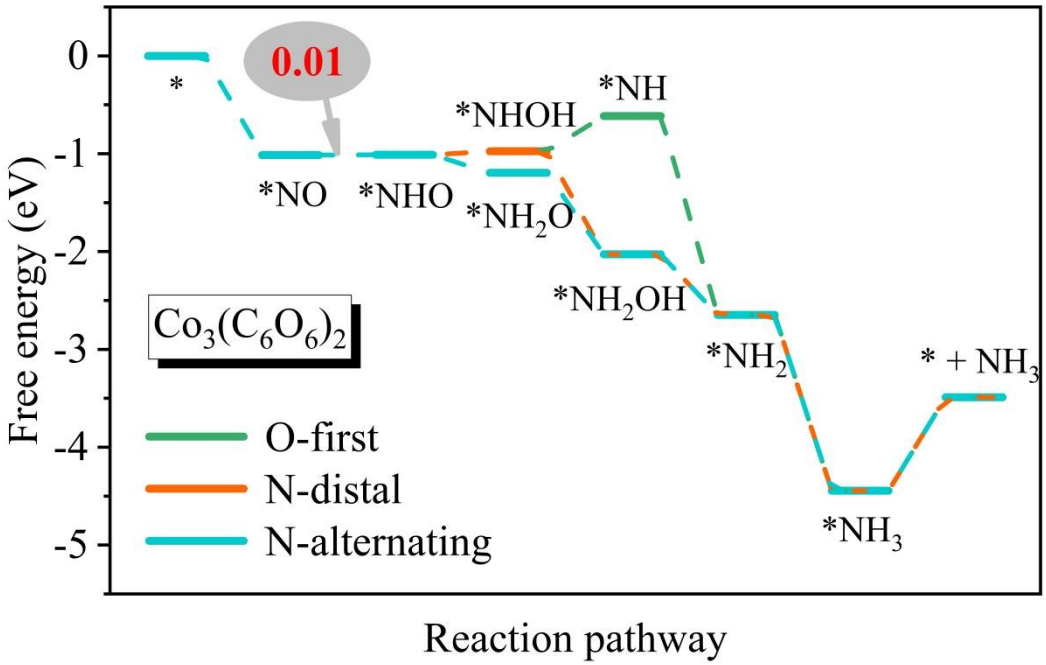

Fig. S4. The free energy diagram of NO reduction to NH_3 on $Co_3(C_6O_6)_2$.

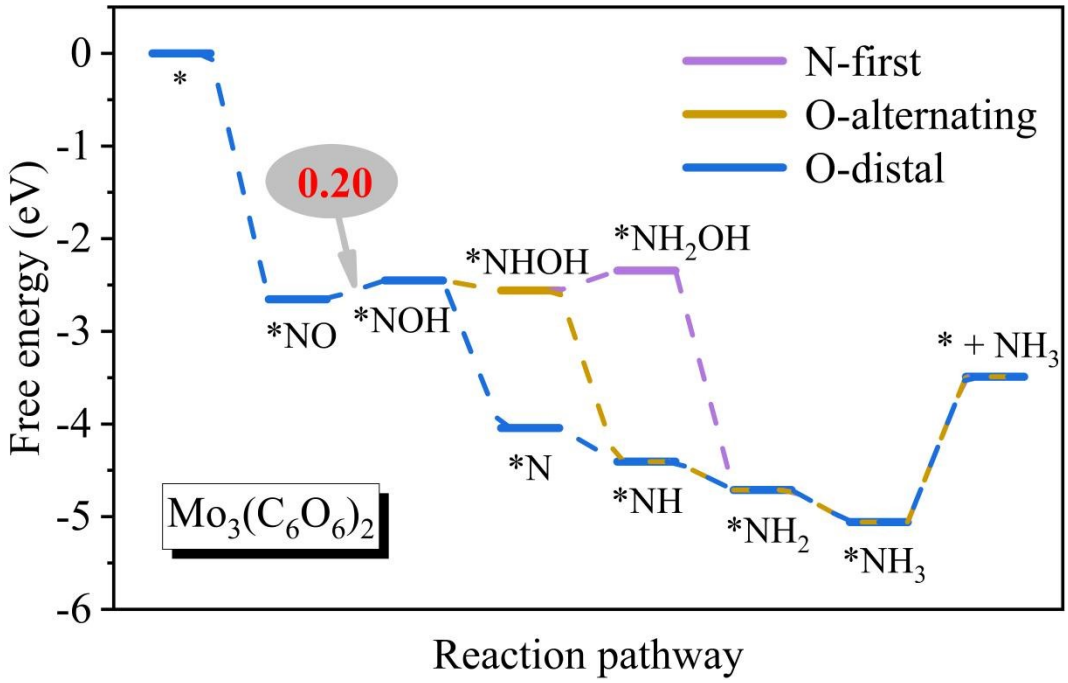

Fig. S5. The free energy diagram of NO reduction to NH_3 on $Mo_3(C_6O_6)_2$.

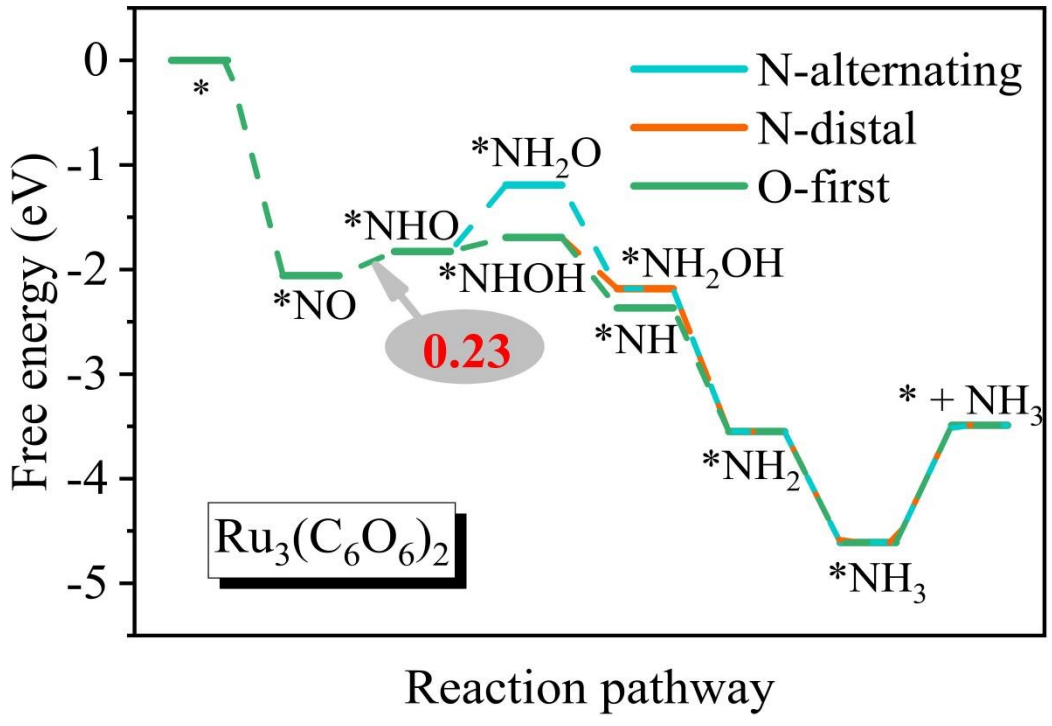

Fig. S6. The free energy diagram of NO reduction to NH_3 on $Mo_3(C_6O_6)_2$.

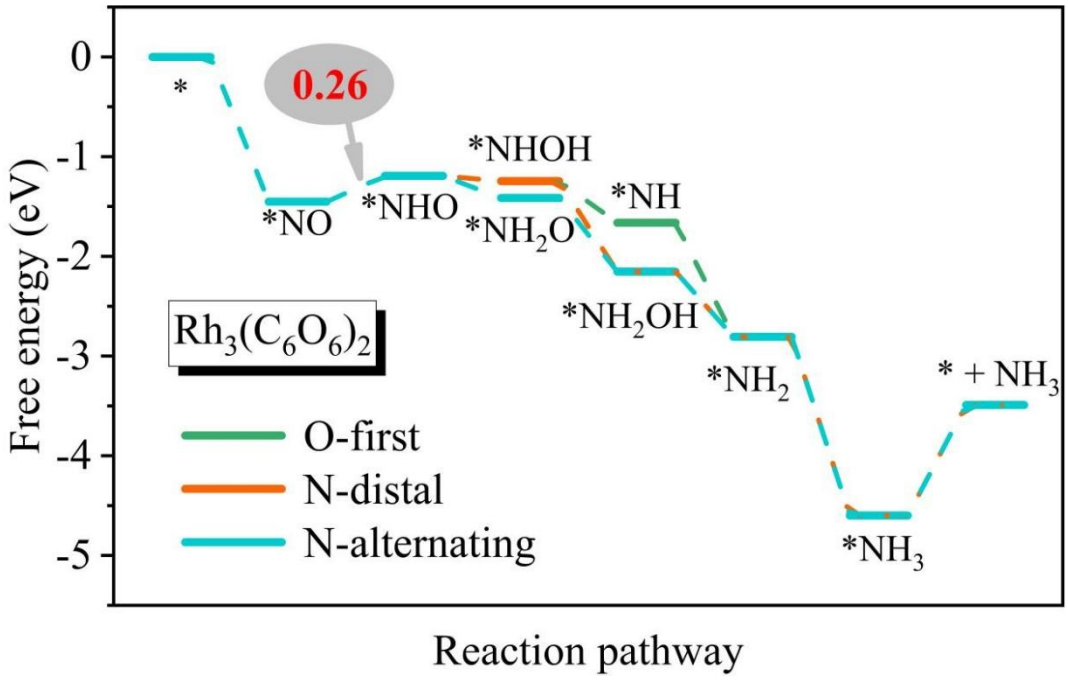

Fig. S7. The free energy diagram of NO reduction to NH_3 on $Rh_3(C_6O_6)_2$.

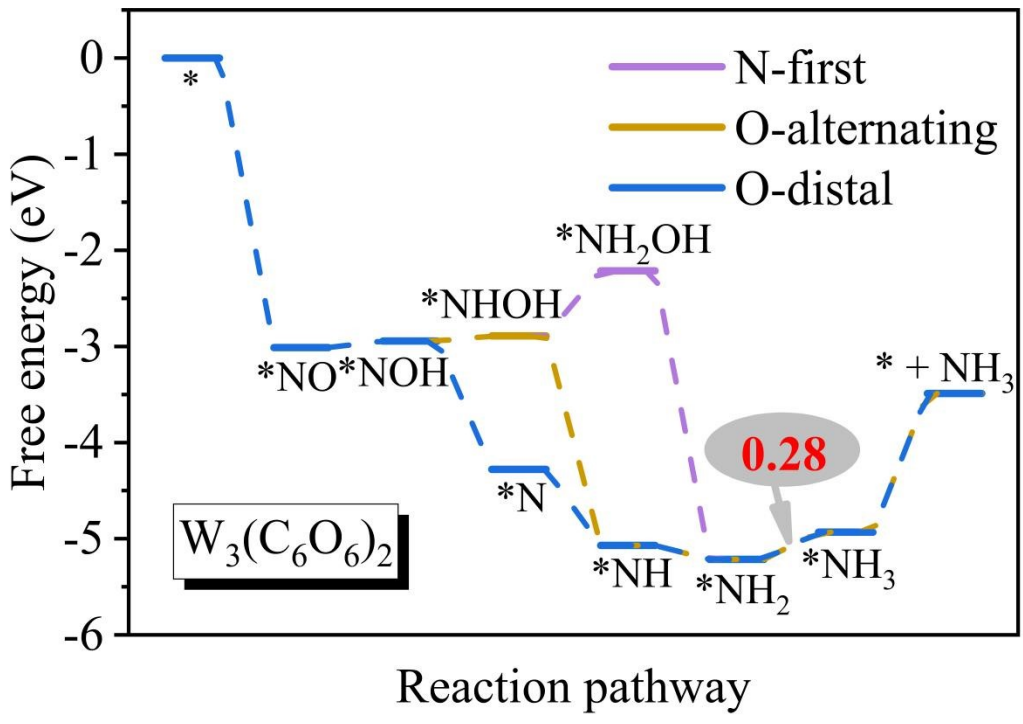

Fig. S8. The free energy diagram of NO reduction to NH_3 on $W_3(C_6O_6)_2$.

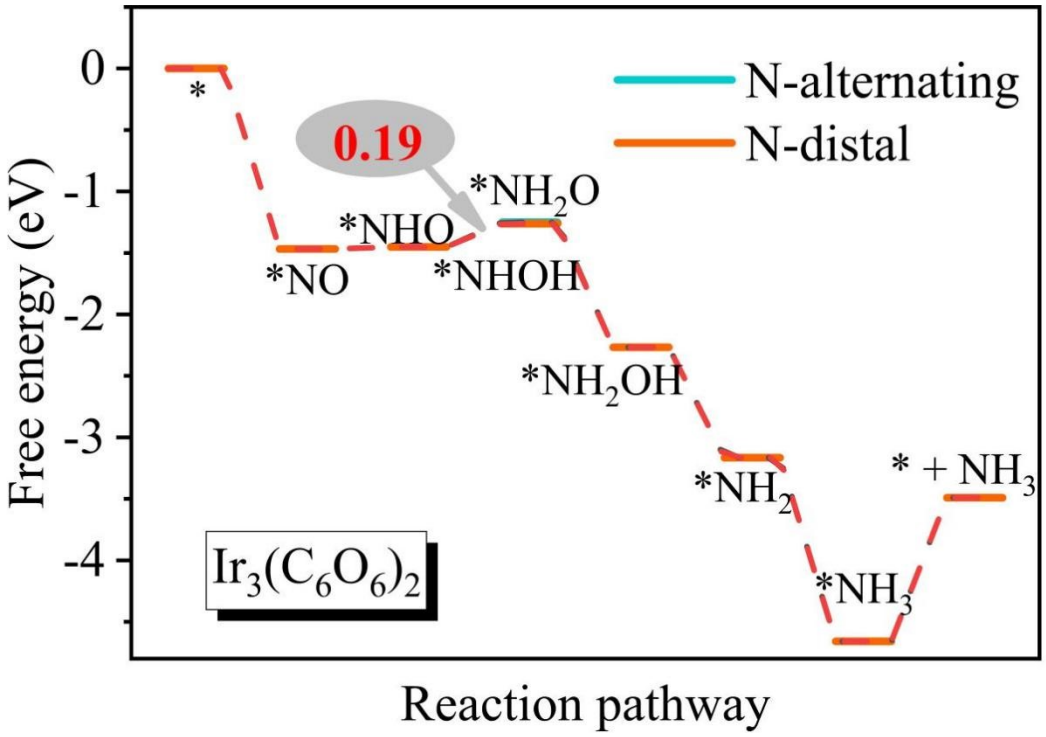

Fig. S9. The free energy diagram of NO reduction to NH_3 on $Ir_3(C_6O_6)_2$.

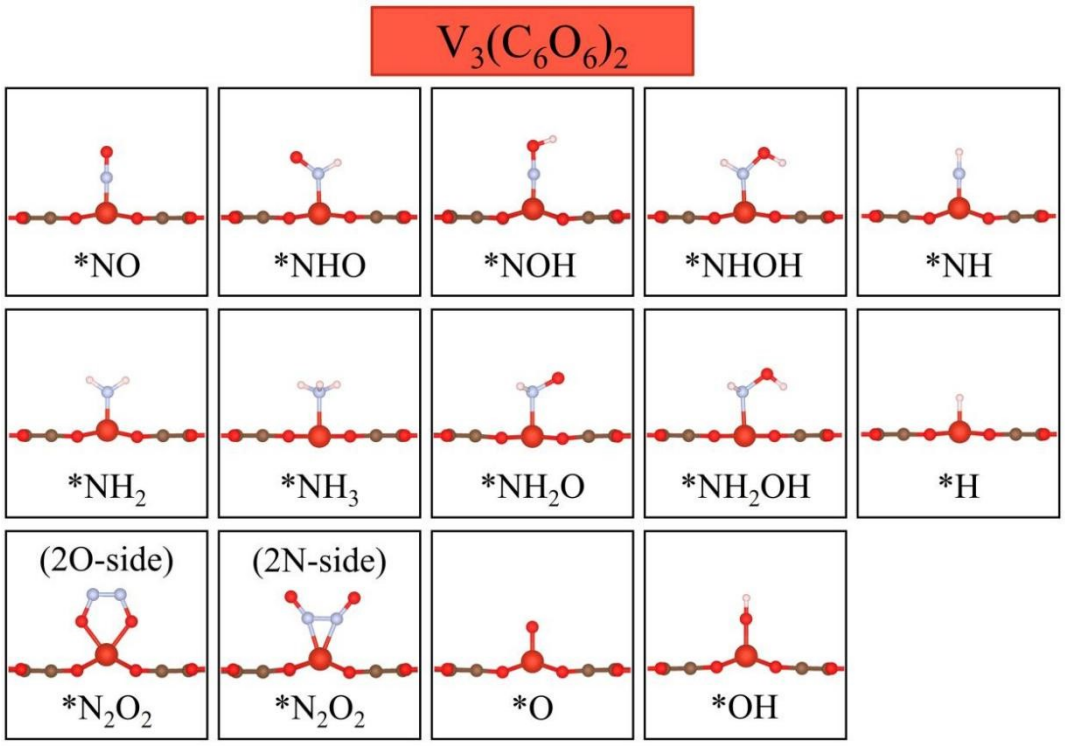

Fig. S10. Optimized intermediates of the NORR via different pathways on $V_3(C_6O_6)_2$.

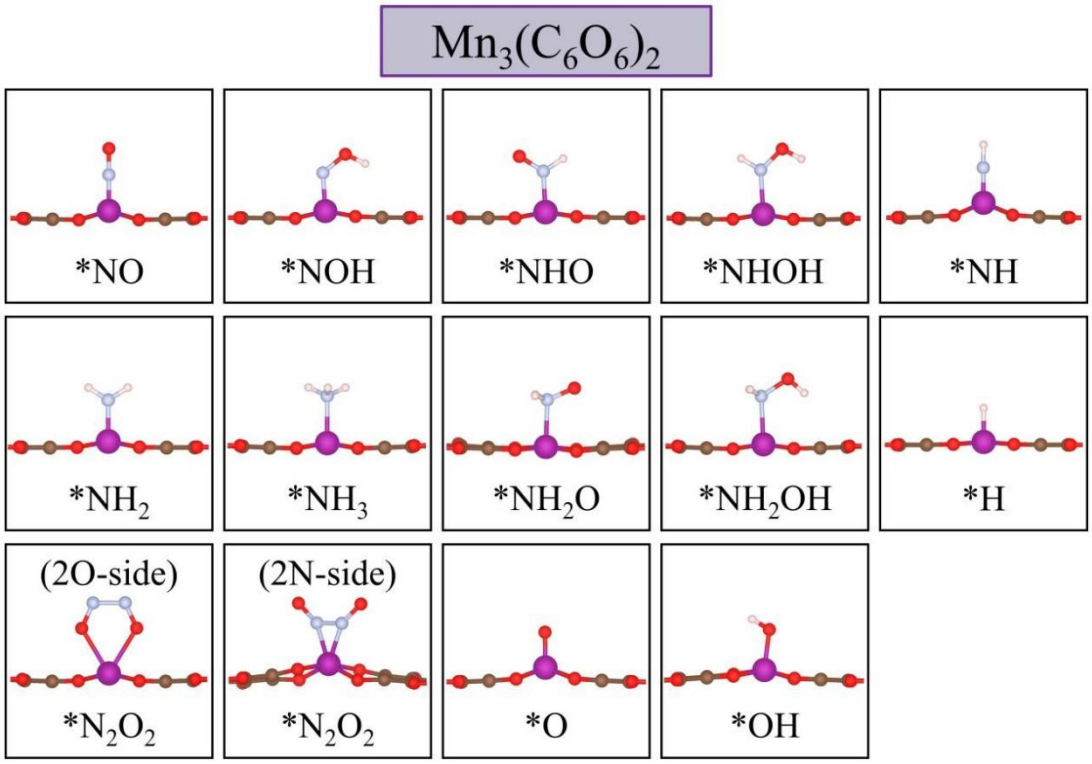

Fig. S11. Optimized intermediates of the NORR via different pathways on $Mn_3(C_6O_6)_2$.

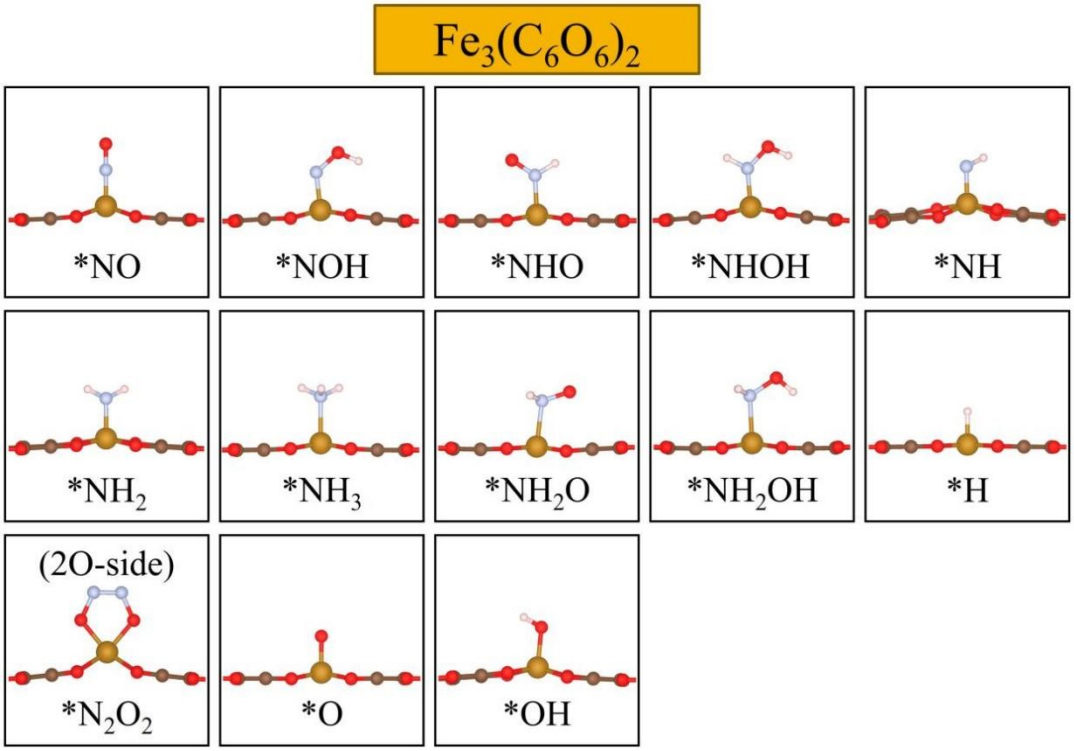

Fig. S12. Optimized intermediates of the NORR via different pathways on $Mn_3(C_6O_6)_2$.

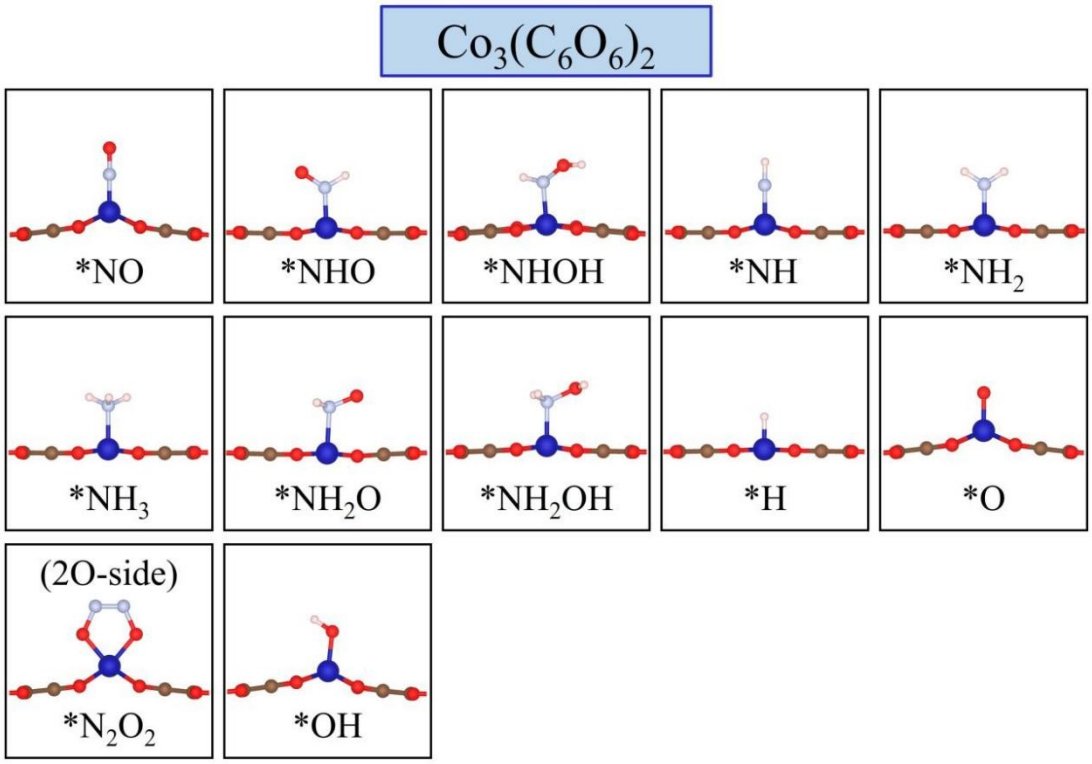

Fig. S13. Optimized intermediates of the NORR via different pathways on $Co_3(C_6O_6)_2$.

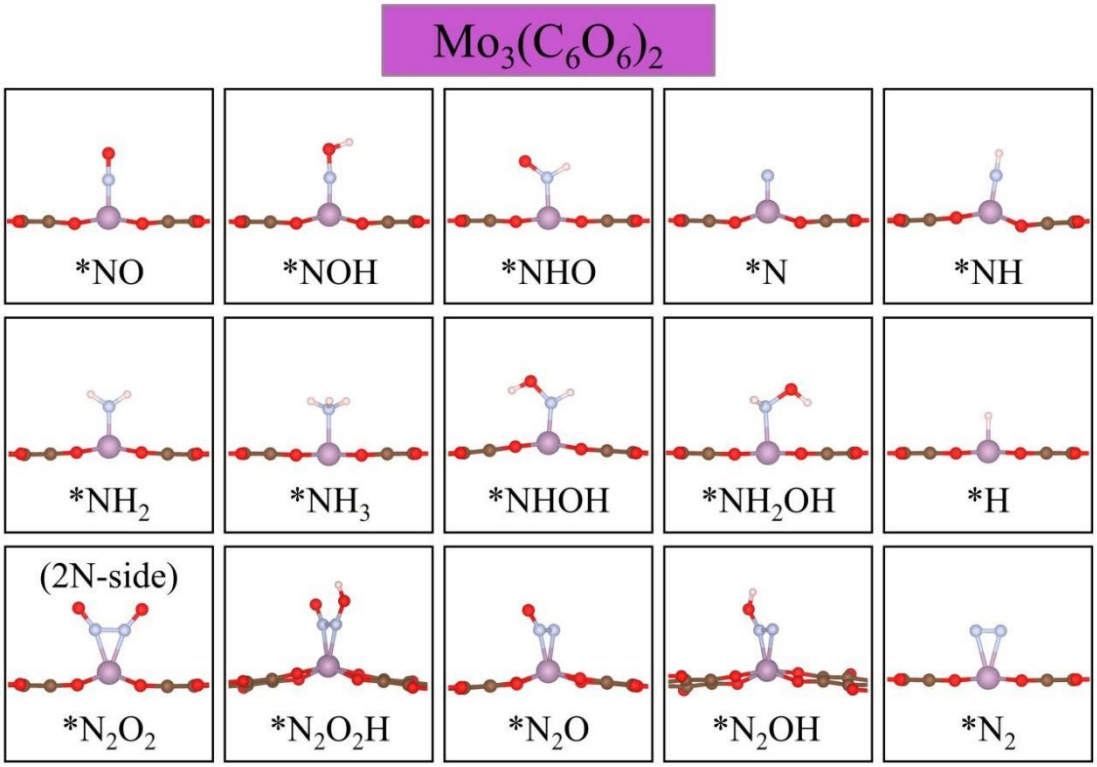

Fig. S14. Optimized intermediates of the NORR via different pathways on $Mo_3(C_6O_6)_2$.

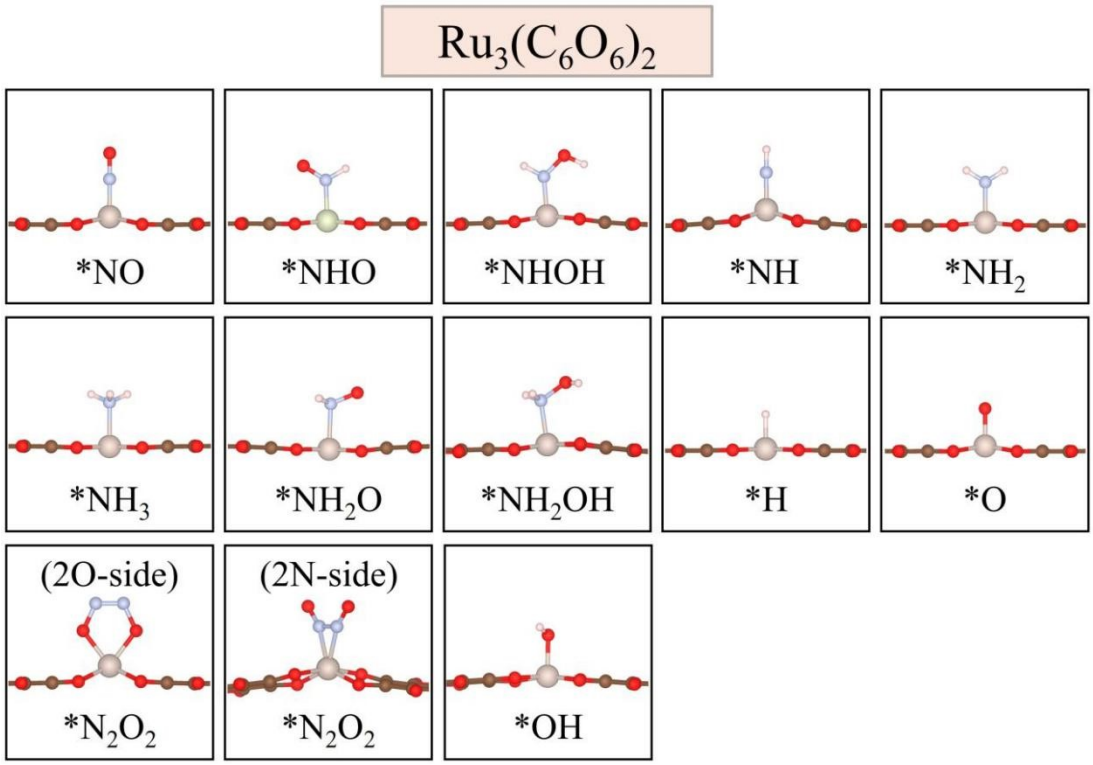

Fig. S15. Optimized intermediates of the NORR via different pathways on $Ru_3(C_6O_6)_2$.

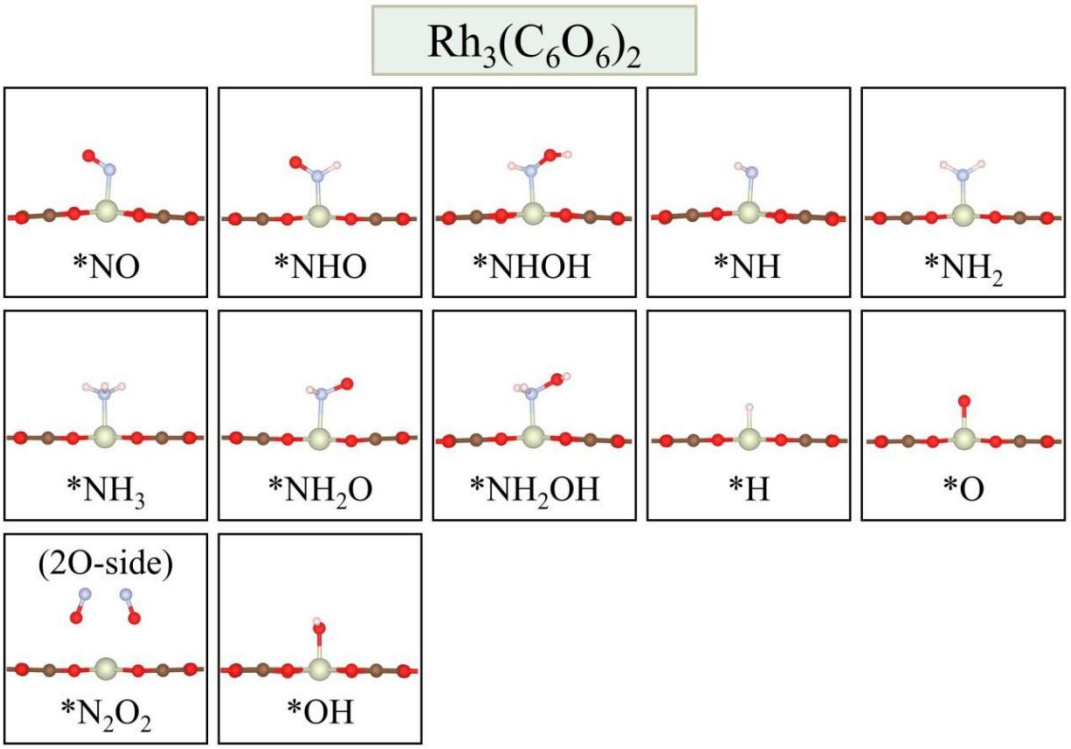

Fig. S16. Optimized intermediates of the NORR via different pathways on $Rh_3(C_6O_6)_2$.

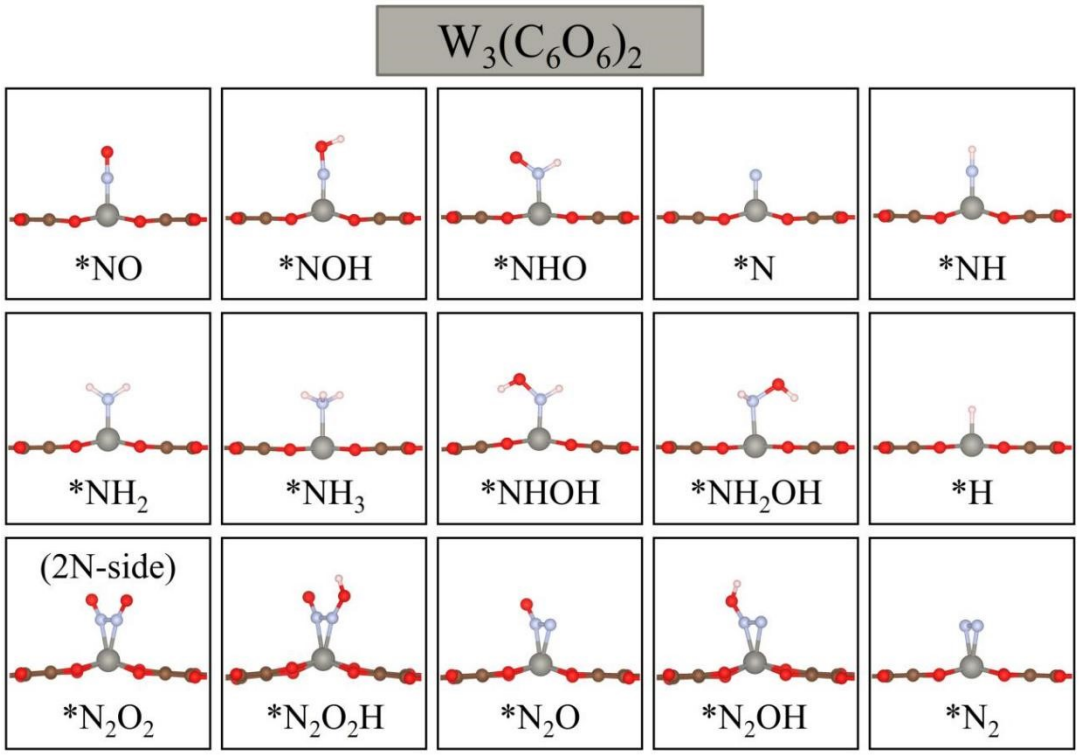

Fig. S17. Optimized intermediates of the NORR via different pathways on $W_3(C_6O_6)_2$.

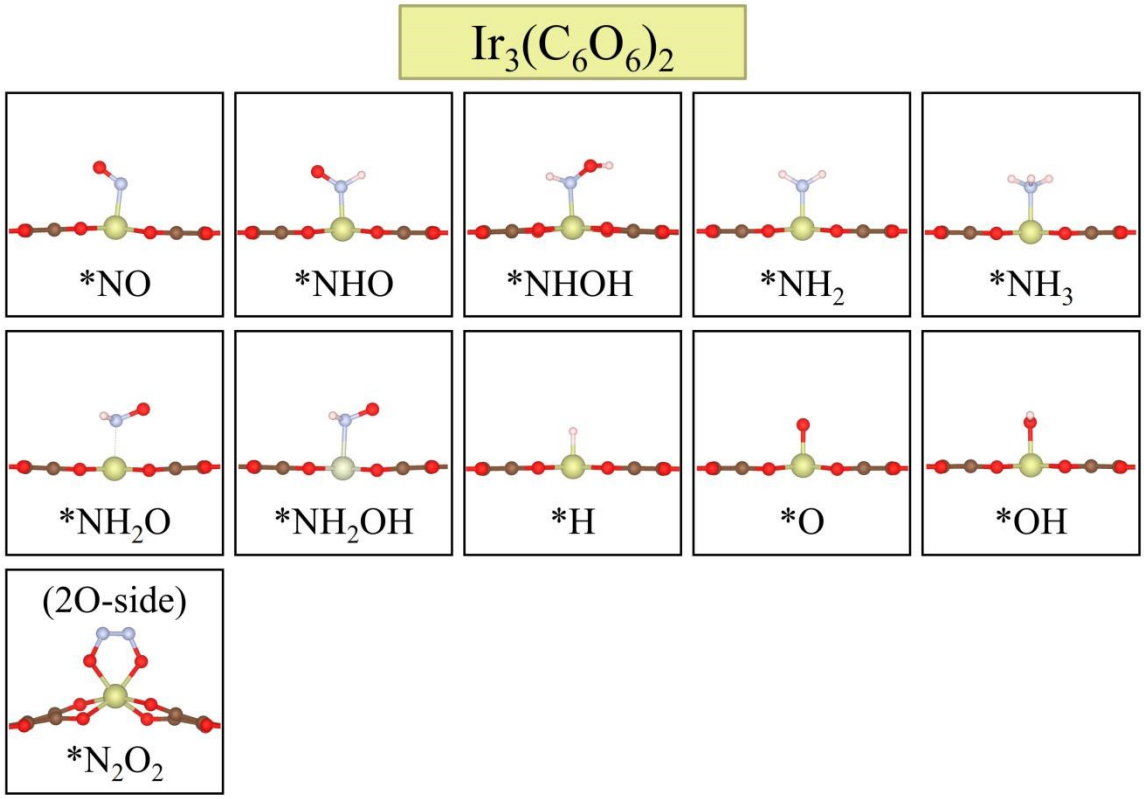

Fig. S18. Optimized intermediates of the NORR via different pathways on $Ir_3(C_6O_6)_2$.

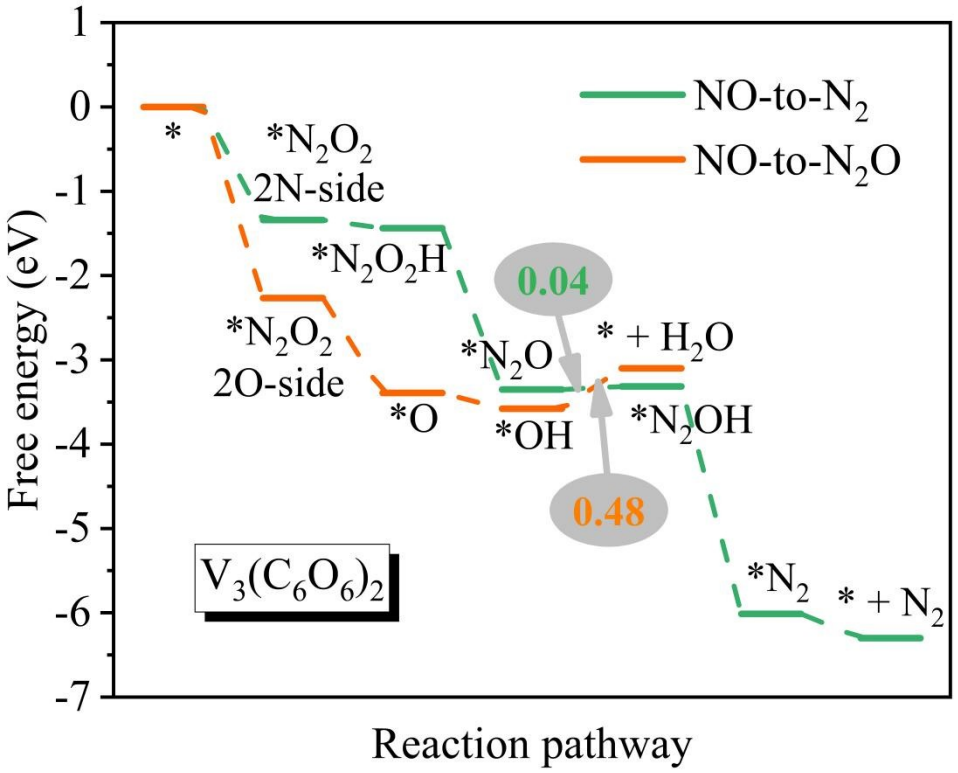

Fig. S19. The free energy diagram of NO reduction to N_2O and N_2 on $V_3(C_6O_6)_2$.

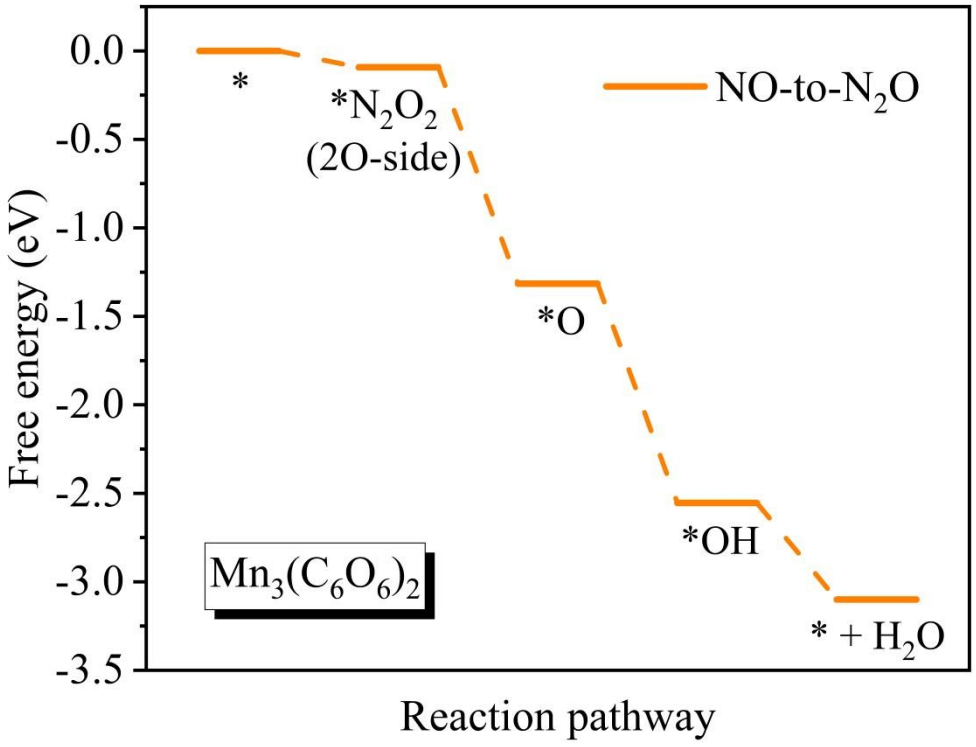

Fig. S20. The free energy diagram of NO reduction to N_2O on $Mn_3(C_6O_6)_2$.

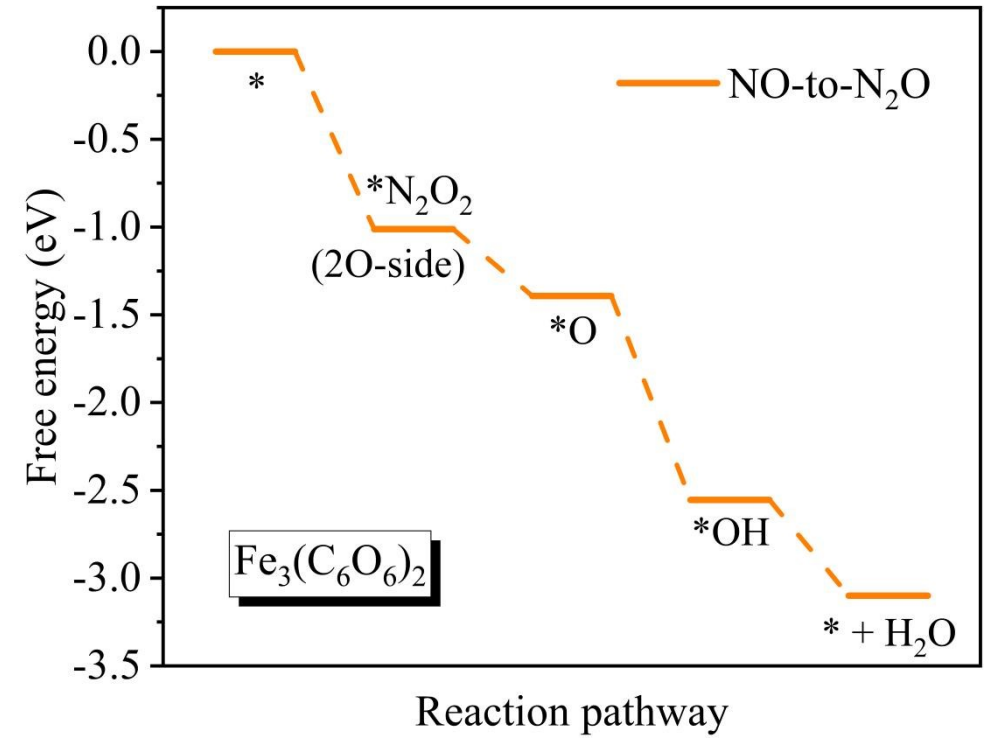

Fig. S21. The free energy diagram of NO reduction to N_2O on $Fe_3(C_6O_6)_2$.

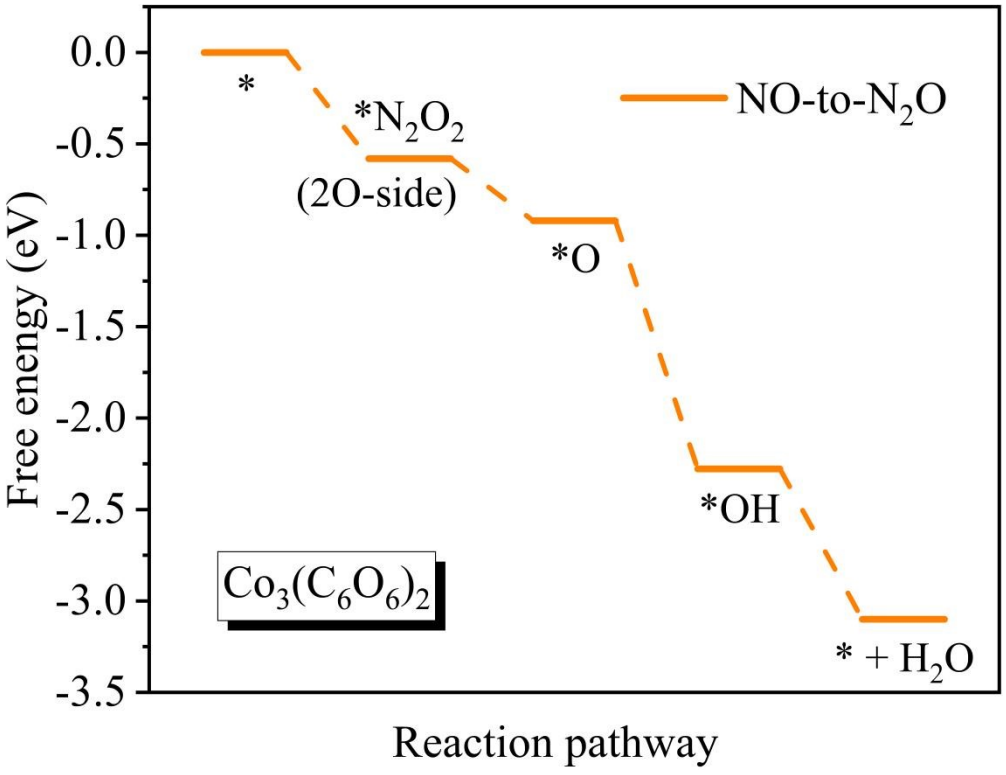

Fig. S22. The free energy diagram of NO reduction to N_2O on $Co_3(C_6O_6)_2$.

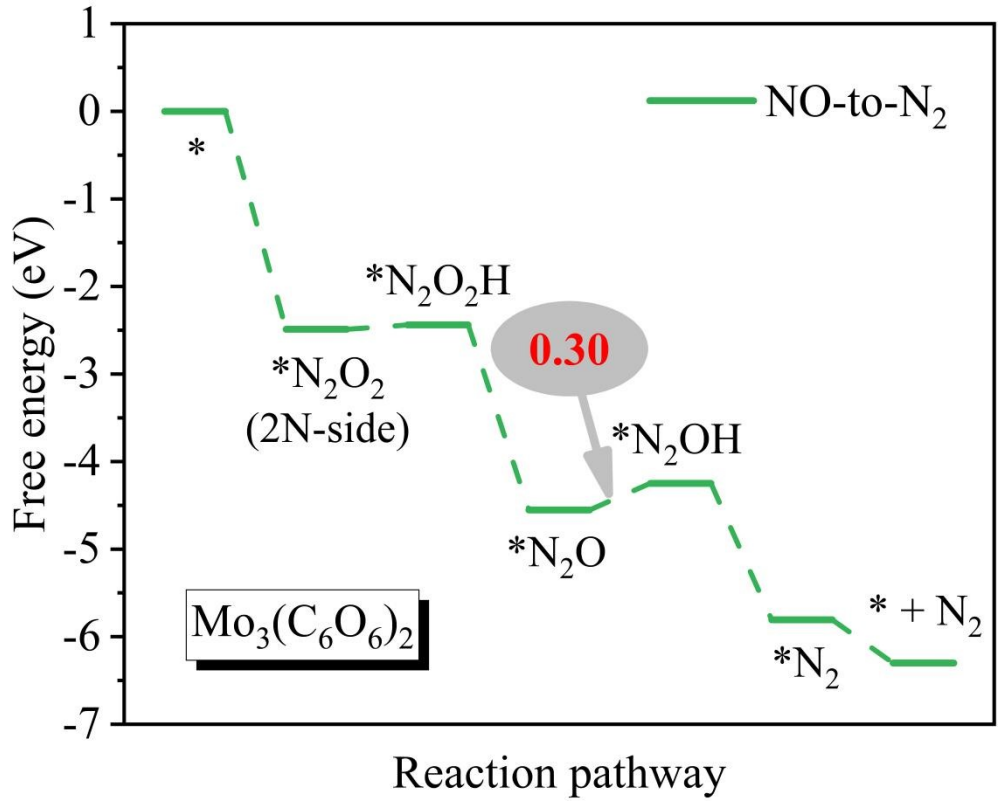

Fig. S23. The free energy diagram of NO reduction to N_2 on $Mo_3(C_6O_6)_2$.

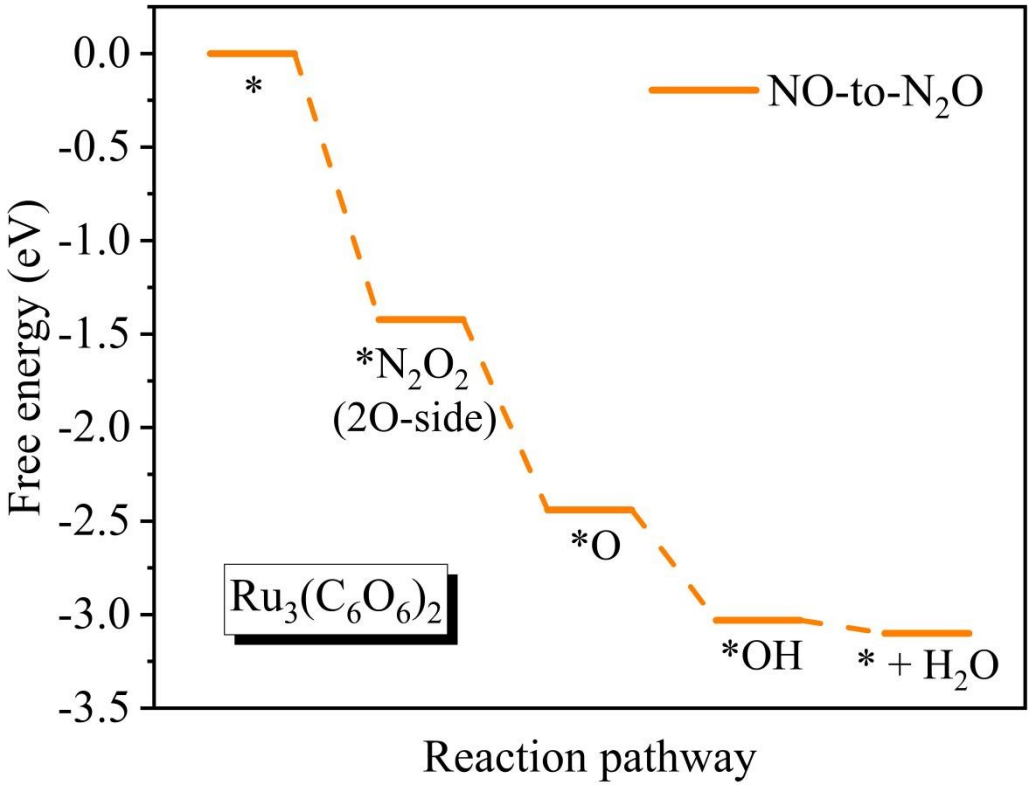

Fig. S24. The free energy diagram of NO reduction to N_2O on $Ru_3(C_6O_6)_2$.

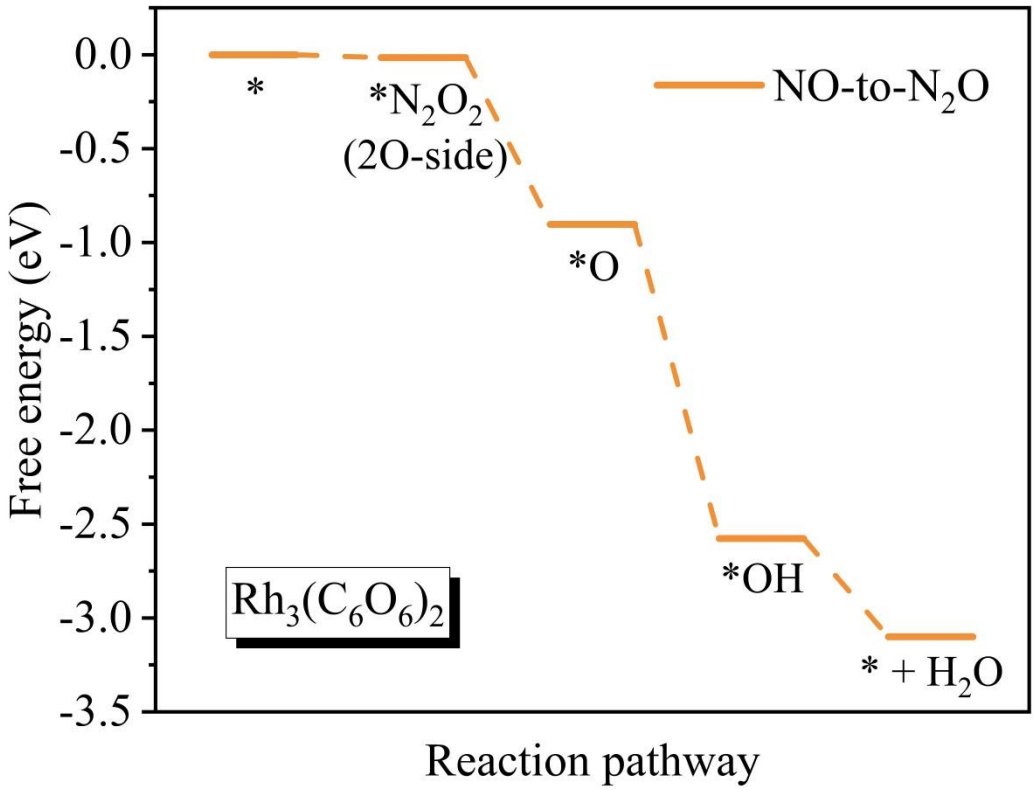

Fig. S25. The free energy diagram of NO reduction to N_2O on $Rh_3(C_6O_6)_2$.

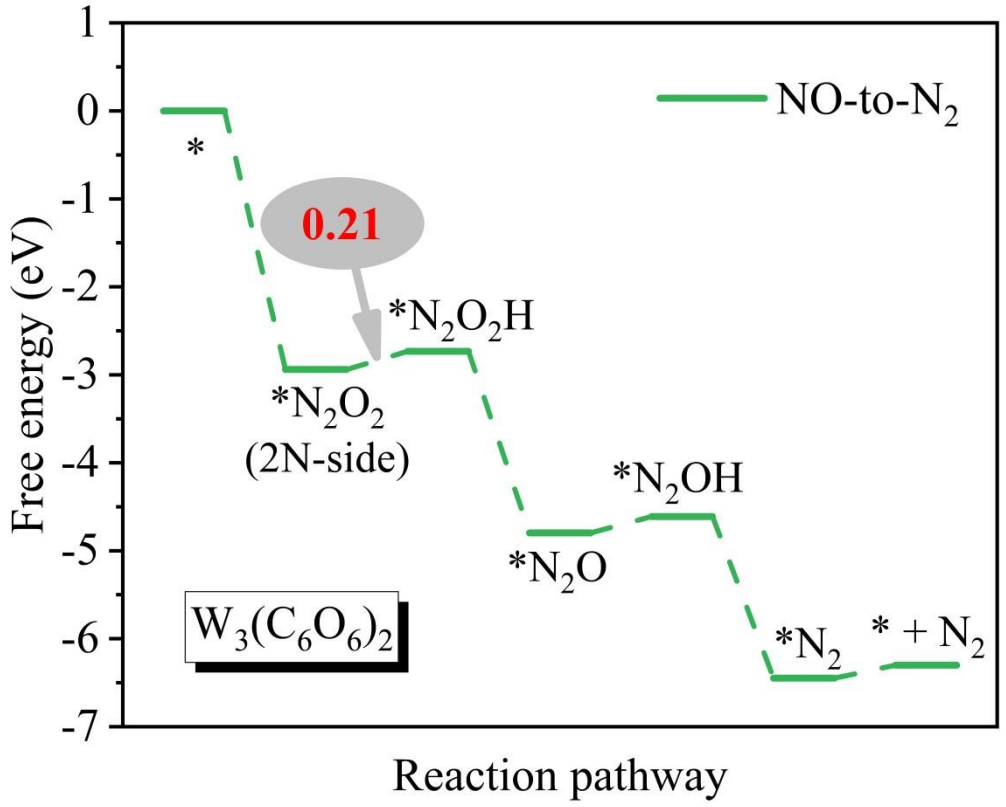

Fig. S26. The free energy diagram of NO reduction to N_2 on $W_3(C_6O_6)_2$.

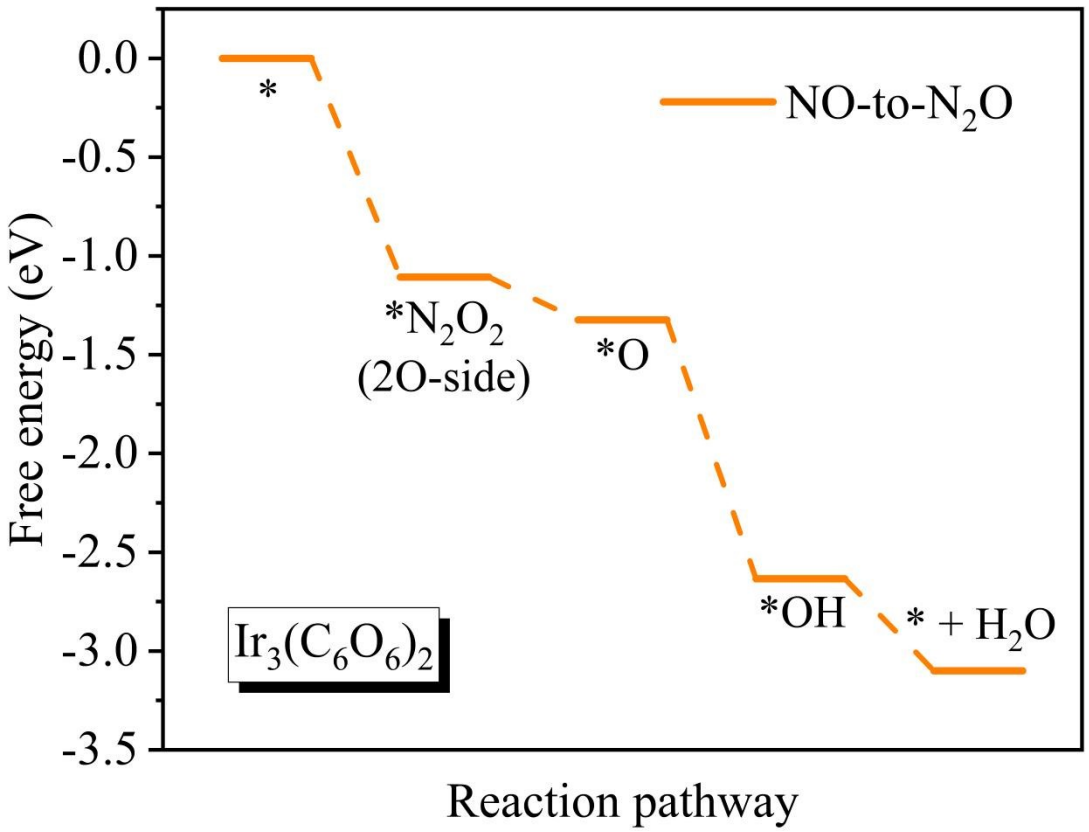

Fig. S27. The free energy diagram of NO reduction to N_2O on $Ir_3(C_6O_6)_2$.

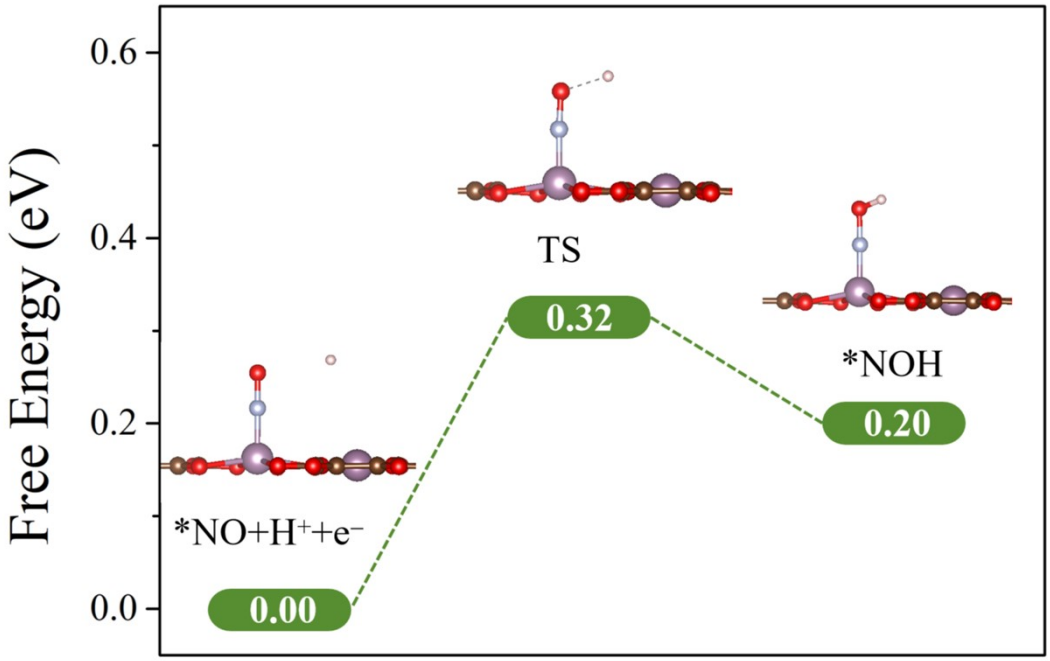

Fig. S28. Kinetic barriers and corresponding atomic structures of the potential limiting step along the most favorable reaction pathways for $Mo_3(C_6O_6)_2$.